MDPI sensors

Article

A Secure Communication in IoT Enabled Underwater and Wireless Sensor Network for Smart Cities

Tariq Ali [1,*], Muhammad Irfan [1], Ahmad Shaf [2], Abdullah Saeed Alwadie [1], Ahthasham Sajid [3], Muhammad Awais [4] and and Muhammad Aamir [2]

1 Electrical Engineering Department, College of Engineering, Najran University, Najran 61441, Saudi Arabia; miditta@nu.edu.sa (M.I.); asalwadie@nu.edu.sa (A.S.A.)

2 Department of Computer Science, COMSATS University Islamabad, Sahiwal Campus, Sahiwal 57000, Pakistan; ahmadshaf@cuisahiwal.edu.pk (A.S.); muhammadaamir@cuisahiwal.edu.pk (M.A.)

3 Department of Computer Science, Faculty of ICT, Balochistan University of Information Technology Engineering and Management Sciences, Quetta 87300, Balochistan, Pakistan; ahthasham.sajid@buitms.edu.pk

4 School of Computing and Communications, Lancaster University, Bailrigg, Lancaster LA1 4YW, UK; m.awais11@lancaster.ac.uk

* Correspondence: taishaq@nu.edu.sa

check For updates

Received: 24 June 2020; Accepted: 30 July 2020; Published: 2 August 2020

Abstract: Smart cities are getting more popular these days. Due to this, Internet of Things (IoT) facilitated Underwater and Wireless Sensor Networks (I-UWSN) are primarily used to analyze and explore the environment with the support of intelligent devices, such as smart cities. In order to increase the reliability of communication, radio frequency is often employed for wireless sensor networks, whereas the acoustic medium is utilized in underwater communication data transmission. The selection of numerous nodes' trustworthy pathways towards the sink nodes and an effective network structure are thus still some of the I-difficult UWSN's concerns. Time Based Reliable Link (TBRL), an unique routing protocol for dynamic topology, is suggested in this study to serve smart cities. TBRL operates in three stages. Using a topology discovery mechanism, it identifies the topology of every node in the network domain in the first stage. In the second stage, the two-node reliable model for a smart grid environment was used to assess the consistency of each formed link. The probability of horizontal and deeper level node-to-node communication is decreased by this consistency model, which also chooses subsequent trustworthy forwarders. The most consistent path is chosen to transfer datagrams after all paths have been investigated in the third step. A network simulator tool is used to manipulate TBRL (NS-2 AquaSim). To evaluate the performance of a system in terms of end-to-end delay, datagram delivery rate and power usage, the TBRL is come up over other well-known routing protocols, such as Depth Based Routing (DBR) and Reliable Energy-efficient Routing Protocol (R-ERP2R). Moreover, the consistency of TBRL is analyzed with that of 2H-ACK and 3H-RM. According to the simulation findings, TBRL works around 15% good than DBR and 10% better than R-ERP2R in perspective of the previously stated performance criteria.

Keywords: topology discover; reliable; consistency; routing protocol; smart cities

1. Introduction

As the trend of smart cities and the environment keeps going up, the Internet of Things (IoT) has emerged as the dominant innovation. The Internet of Things (IoT) was first used, as far as we can tell, in 1999 (https://www.postscapes.com/iot-history/). This is referred to as the information society's architecture (accessed on June 18, 2020).IoUT is a network of intelligent, linked underwater artifacts, also known as IoT-enabled Underwater and Wireless Sensor Networks

(I-UWSN s). Autonomous Underwater Vehicles (AUVs), buoys, ships, watchman nodes, etc. are examples of various categories of smart objects that include sensors. I-UWSN architecture is a special variant of IoT as a result, and it is anticipated to serve a number of real-world uses including crisis mitigation, environmental monitoring, and underwater investigation. I-UWSN is viewed as one of the technologies that might contribute to the growth of smart cities because of these utilizations. [1,2].

Because of a number of factors, I-UWSN is attracting the interest of researchers and academics. The fact that the Earth is around 71 percent covered in water and that only about 10 percent of it has been explored is one of the key causes. As a result, it is a cutting-edge technology that holds the potential of ocean environmental research and monitoring. In I-UWSN, sensor nodes can be set up in a variety of ways to achieve the legitimate goal. Nodes may be arranged in a grid or a tree-like layout, or they may be distributed arbitrarily. First, each sensor node has the computing, communication, and cognitive skills to cope with an intelligent environment, such as in smart cities, in order to deliver reliable data transmission [3,4]. The data is then flooded toward the destination address by nodes when they have sensed it. Modern I-UWSN implementations include those for environmental research, crisis warning, aided direction, resource exploration, and military needs [4–6].

For the given uses, a number of routing protocols have been offered. Due to the special parameters of the transmission medium, such as the confined bandwidth caused by the usage of the acoustic channel, existing terrestrial network routing techniques cannot be employed in underwater and smart city communication [7,8]. Since the speed of an acoustic medium is five orders of magnitude slower compared to radio signals, underwater environments have five times more propagation delay than terrestrial ones. When batteries can't be recharged often, high bit error rates and brief connection losses (shadow zones) might happen, which reduces battery power [9–11]. To address these issues, various I-UWSN routing methods are put forth, utilizing the benefits of undersea features. The strengths and weaknesses of every paradigm are both reflected. As a result, I-UWSN is actively researching routing protocol design and implementation in order to support the concept of smart cities. Lastly, the routing protocol must guarantee the efficacy and accuracy of the data transfer from the source to the target node. The program objectives can be met, or they can lead to the proper judgments or paths, in support of reliability. Consequently, WSN or I-UWSN both offer the dependable communication needed for any application. [12]. Building a dependable application is difficult on both networks. Sensor nodes in the I-UWSN travel between one and four m / sec due to water currents, which include changes in water pressure, humidity, saltiness, and the motion of water bodies. These motions necessitate the dynamic topology combating the factors lowering routing dependability [6,13]. In [14], the dependability of data Forward Error Correction (FEC) and re-transmission-based schema are raised by two new methods. The transmission of datagrams is given additional redundancy in FEC, meanwhile the receiver ask for retransmission of information is met by Automatic Repeat Request (ARQ), which retransmits the unsuccessful packet.

Network topology, which is acquired via a reliable link, influences the network's energy utilization, bandwidth, and transmission latency. [15]. The three components of a stable link are packet-based (all formed packets are consistent), event-based (all formed actions for the routing process are consistent), and sum of packet event (packets generated from a source node by maintaining a reliable link towards destination node) [14]. A proficient connection must be taken into account while choosing the route with the highest likelihood of success [16,17]. Because smart cities are becoming ever more popular, environmental detection systems and algorithms are in great demand. In this research, we present a cutting-edge protocol called Time Based Reliable Link (TBRL), where the influence of dynamic topology is minimized by using a distance-based reliability mechanism. The optimum route for transmitting data is chosen by the TBRL, which evaluates the connection quality for all currently used routing pathways between the origin and destination. In TBRL, a dynamic and dependable technique for seeking a path that is more trustworthy in terms of information, energy, latency, and output is taken into account by taking use of scarce funds.

The planned TBRL is anticipated to provide the following results:

- Despite utilizing the Global Positioning System, position-aware routing (GPS).
- Verification of a node-to-node consistency.

- From offshore, any route that may possibly sink is removed. The data transmission follows the affected route.
- Before running the simulations, it is well understood what the channel's expected latency and energy utilization would be.
- TBRL does not need the upkeep of a complicated routing table or the use of additional equipment resources.
- To offer a trustworthy route for interaction among sensors and intelligent devices, TBRL is appropriate for smart environments such as smart cities.
- For the aim of categorizing and identifying underwater artifacts, TBRL aids machine learning techniques.

This paper is arranged as follows: inside Section2, research stuff is provided; The network model is described in Sections 3 and 4 explains what the mathematical analysis says; in the Section5, the simulation's outcomes are discussed. Ultimately, we concluded in Section6.

2. Related Work

In the past ten years, a number of routing protocols have been suggested to provide consistent transmission in both underwater and intelligent surroundings. A Self-Organized Underwater Wireless Sensor Network (SOUNET) is suggested in order to overcome the problems of network recovery latency and design complexity, related to [2]. In order to place nodes, tree topology is used. Each node receives a variable ip for authentication, number of hops, or hierarchical level. Just a primary ip is necessary to add a new node at any level. Additionally, it resolves the closed loop and node isolation issues, however SOUNET is not strong enough to maintain dependable interaction throughout a lengthy route. In [3], a thorough explanation of region segmentation and localization-free UWSNs routing methods is covered. Region segmentation protocols, in contrast to localization-free methodologies, require network knowledge prior to routing. Every routing system created for underwater environments has its own restrictions in terms of dependability, latency, datagram losses, and bandwidth problems. The authors of [5], give a thorough analysis of the UWSNs programs already in use, along with the potential and difficulties associated with their implementation in the UWSNs context. The information from the currently submitted requests was collated and grouped into five main categories, each of which was further subdivided into pertinent subgroups.

Reliable and Topology Control Protocols in Uwsns

In [4], The routing protocol known as Topology Efficient Discovery (TED) is presented. TED correctly assesses link integrity while minimizing downtime complexity. TED is associated with time frames designated for transmission, where nodes are given a designated time slot in order to send a datagram or a number of datagrams. It also facilitates finding node pairings whose distribution is obstructed by utilizing the innovative Near-Far Node Pairs (NFNPs) technique. In [8], Analytical work to assess the integrity of the relationship is presented. Any UWSNs system's dependability can be examined using their methodology. Their scheme facilitates the Code Division Multiple Access (CDMA), Multiple Input Multiple Output (MIMO), and Binary Phase Shift Key (BPSK) communications networks. In [14], To increase the data reliability of multi-hop UWSN, end-to-end and hop-by-hop erasure programming are considered. For the routing procedure, the Depth Based Routing (DBR) protocol is employed. Without any positioning data, DBR has an effective method for managing the system constantly.

In [16], For topology control in different reportage, the algorithms traversal and radii incremental are offered. In the traversal strategy, only the sensing node expands its radius at each round, however in the radii incremental approach, the radii of many nodes simultaneously increase at each round.

In [17], For utilizing link accurate data, the Channel Aware Routing Protocol (CARP) is introduced. Only nodes with a successful track record of transmitting data to their neighbors are chosen for data forwarding. Links of this caliber are so exploited. For network topology management, hop count is used. In [18], The authors propose a power management strategy to enhance the

lifespan of the network and functionality. In order to determine the best approach, they employed a local pattern search engine and a genetic automated process meta-heuristic searching for the global design area.

In [19], I-UWSN node power consumption is balanced by considering mobility of nodes and a spherical energy minimization model. Their model also regulates datagram duplication and route gaps. Additionally, they have discussed the exchange between energy conservation and information delivery dependability. In [20], The underwater atmosphere makes the audio communication unstable due to a high return loss and a gap issue. Cooperation between intermediary nodes for datagram forwarding is employed to get around this problem. A limited heuristic search is used to determine the optimum forwarding path. In [21], an effective and dependable technique based on remaining energy data, communication range, and actual distance data. End-to-end delay, network longevity, energy usage, and delivery ratio are all considered to have significantly improved over their prior work. A comparison of a few cutting-edge routing methods is also provided in Table1.

Table 1. Comparison with cutting-edge routing protocols

Protocol Name	Weakness	Proposed TBRL
GEDAR [22]	The selection of neighboring sets has some trade-offs due to its greedy approach mechanism	It does not support greedy approach, it accepts node by calculating reliability inn term of expected transmission count, residual energy, and distance in between them.
DCR [23]	For every time the depth is calculated for flooding, so large end-to-end delays occurred	At initial stage, TBRL determines the depth of each node create possible paths to avoid large end to end delay
SWARM-SEA [24]	The scheme runs in hybrid mode (DCR+GEDAR), and complexities are increased to detect in underwater nodes movements	It proposed algorithm for detecting the nodes movement to reduce the complexity in term of computational cost
VARP [25]	Longest propagation delay occurs, at every hop count.	It proposed average time calculation process in its mathematical model to reduce propagation delay.
L2-ABF [26]	Before the flooding, each time angle zone is calculated whereas nodes depth not considered for selection of nodes, so the unexpected delays and energy consumption occur	All reliable links are established, and average time calculation is taken, furthermore, specific depth threshold is defined for next node selection. Thus, it helps to measure expected delay and energy consumption.
AHH-VBF [27]	Consumption of battery issues are highly affected	Energy consumption model is provided for the approximate energy utilization of network
NADEEM [28]	Low network throughput, fails to find another routing path when the void nodes are present on a dedicated path	Expected transmission count is considered for the selection of reliable link to maximize network throughput
ASEDG [29]	Link quality and AUVs time for data gathering process not considered, thus unexpected delay occurs.	Link quality is measured for data gathering process and expected delay is measured
DBR [30]	Used greedy approach in term of depth and not considered links quality between nodes	Next node selection based on link quality and depth threshold is defined for routing process

	3H-RM [32]	There is no mechanism introduced for the acknowledgment process when step size is less than 3 thus it makes higher probability of packets duplication at sink node	2N-RM consists of two nodes reliability model and no step size is taken. When data reached at sink node, there is a zero probability of duplication data packet at sink node due to one to one relationship.
	2H-ACK [33]	When second node becomes sink, it has no choice for taking acknowledgment from other receiver and send it to source node	Two nodes ensure the reliability by taking the consideration of ETX value and have proper mechanism to acknowledge the source node.

3. System Model

It is suggested to use the novel routing protocol TBRL for crucial underwater monitoring missions with dynamic topology. In TBRL, solid connections are made between the nodes at various depths. It is a multi-sink topology discovery routing protocol that is dependable, delay-sensitive, energy-efficient, and effective. Data sent from sensor nodes on the water's surface and certain nodes that are moored at the bottom are collected using a number of surface sinks. The remaining nodes are placed at various heights between the ground and the water's surface. Data packets that are based on link quality will be forwarded by the nodes. Any node used for data gathering transmits the data to the following nodes by taking dependability into account. Any of the surface sinks that a data packet reach is regarded as having effectively transported it to its intended location. Figure 1 displays the TBRL flow chart. These sinks can connect with one another at higher bandwidths and with fewer propagation delays thanks to the capability of radio communication.

Three stages make up the three steps by which TBRL completes its communication process:

- dynamic topology discovery algorithm
- two nodes reliable model
- topology changes of existing paths

The position of nodes is determined in phase one by considering their depth and water speed at various depths. By making sure a link is reliable, nodes forward data packets to subsequent nodes or sinks in the second phase. The least affected path is returned in the third step after all potentially reliable paths have been taken as input parameters.

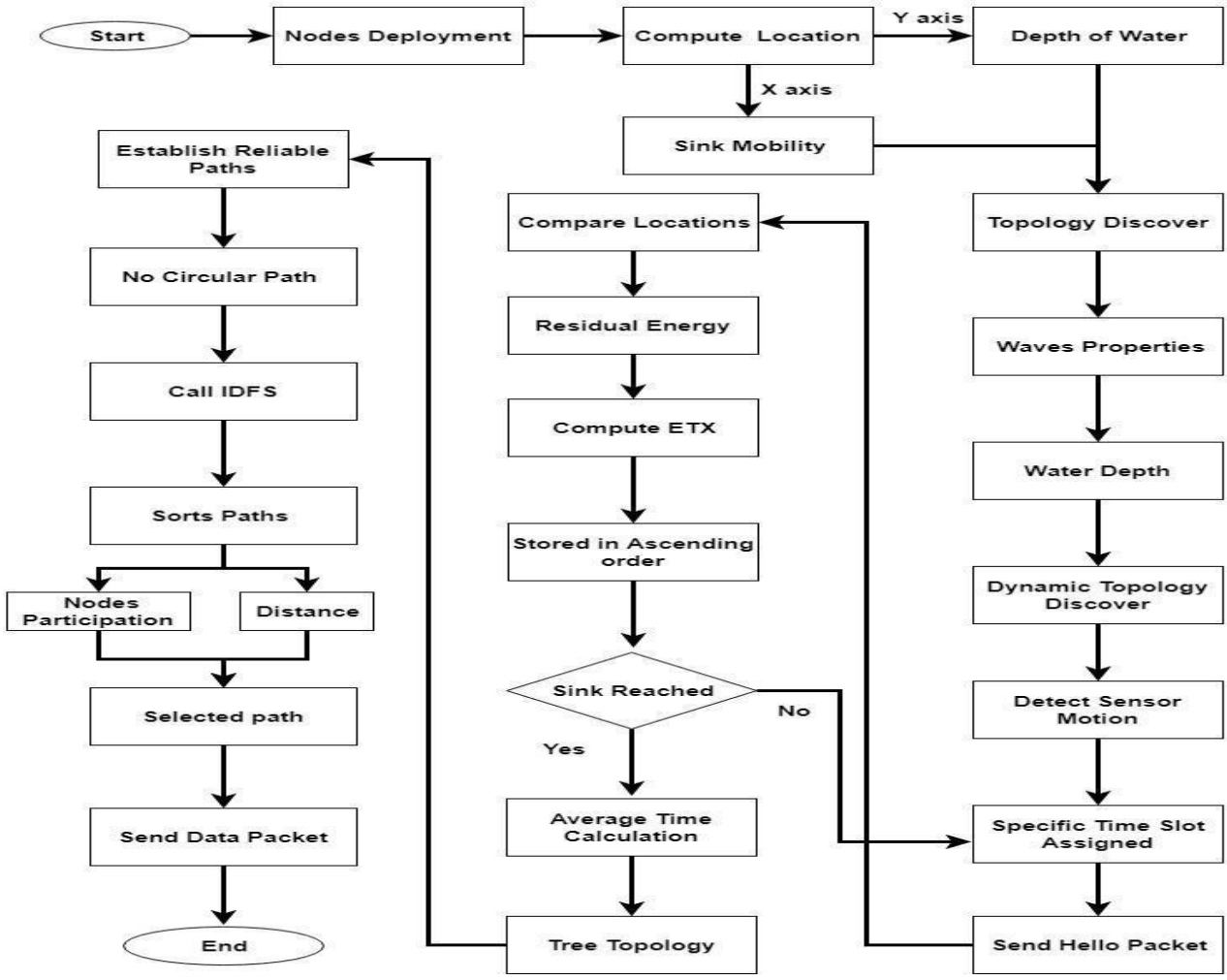

Figure 1. Flow Chart of Time-Based Reliable Link (TBRL).

3.1. Dynamic Topology Discovery Algorithm

A positioned-aware routing protocol is TBRL. In order to determine each node's position, we first assume that its X axis is unknown, and its Y axis is equal to the depth of the water. Each node's X axis moves far more frequently than its Y axis because of the constant flow of water. Additionally, calculating the depth (Y axis) in an oceanic environment is much simpler than calculating the width (X axis). Axis) computation. Figure 2 displays a number of sinks distributed at random and spaced at equal intervals.

Additionally, each sink has been given specific mobility according to the network area from its initial point to its last point, which is also the initial point of the following sink. Sink nodes calculate their movement toward the X axis to travel from their starting location to another point. The Y axis is always 0 and cannot be modified since sink nodes might move horizontally. Because of this, distance always shifts in the X direction.

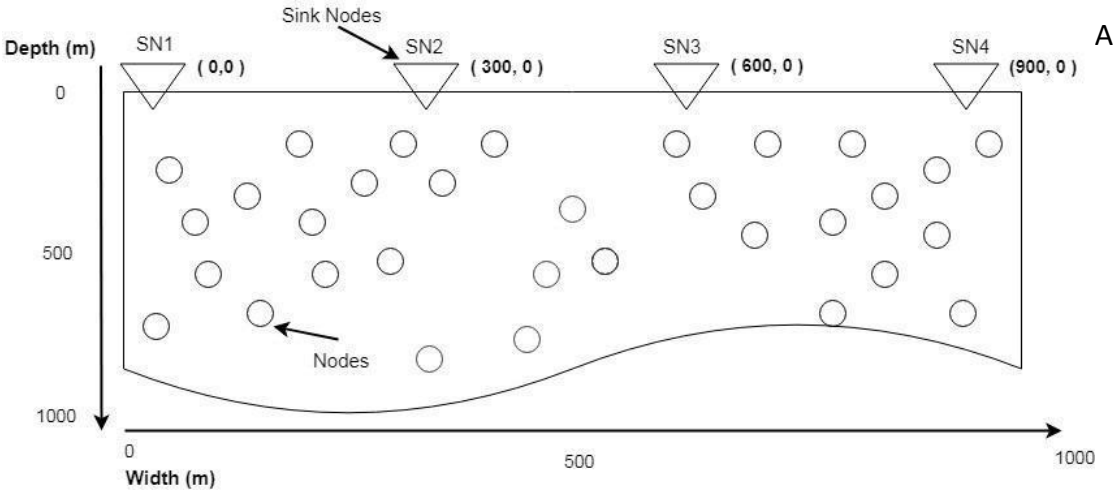

Figure 2. Finding X axis Location

Location Packet (LP) containing the constant value for the X axis is sent vertically. This makes nodes very aware of where they are in relation to the network's X axis. The process of nodes identifying their locations is also shown in Figure 3. With an initial position of (0,0), Sink Node 1 (SN1) will send LP downward by setting the X axis to 0 and raising the value of the Y axis. A node will update its X axis location, which was unknown to it at the time of deployment, if it gets LP. Similar to this, SN1 sends LP at various X axes and modifies the descending node's placement. SN1 may move from 0 to 300 m and then return to its starting place after reaching its destination.

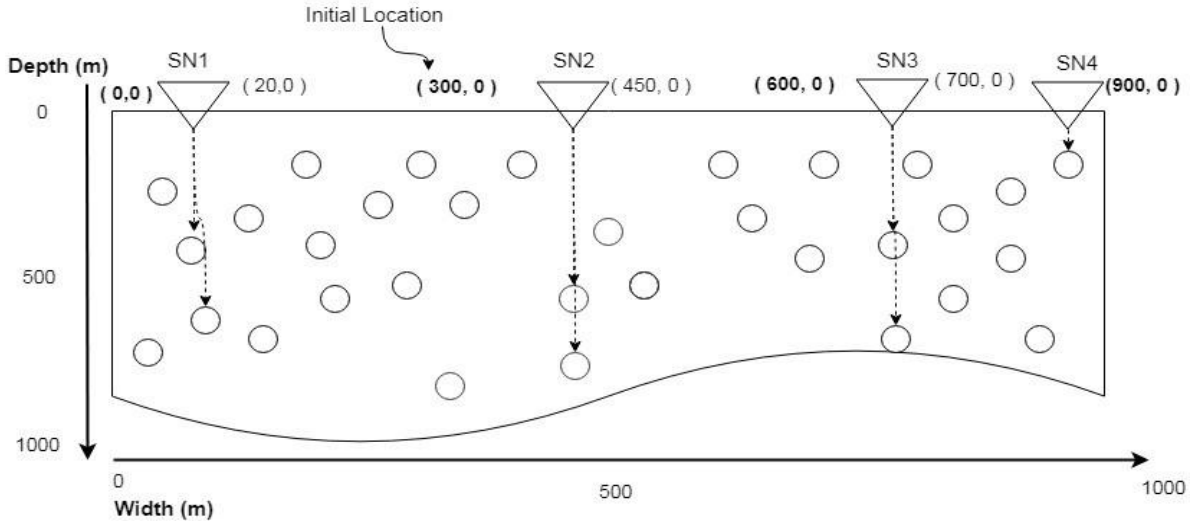

Figure 3. Assigning X axis Location.

Other methods for calculating horizontal distance are inappropriate in this situation. The distance would be smaller or larger at the same depth level; so, Pythagoras theory and angle-based side computation mechanism did not operate effectively in such a tough environment. Instead of GPS, Algorithm1 is presented. Due to the moment of water, nodes move at speeds ranging from 1 to 4 m/s, and this movement changes with depth. Wave theory can help us understand such movement at a deeper level. Waves are classified according to their length, height, and period. Because water waves move in a circular pattern with a crest angle of about 120 degrees. As water depth increases, the wave height decreases and the wavelength increases. As a result, deep water has increased pressure and speed. To compute the speed of water, Fetter and Walecka created Equation (1).

$$\mathbf{speed} = \sqrt{(((gf * \lambda)/(2 * \pi)) * \tanh(2 * \pi * depth/\lambda))} \quad (1)$$

Here, gf indicates force of gravitation, λ indicates wavelength and water depth is represented by depth. For λ Equ(2) is used.

$$\lambda = 1/2 * depth \quad (2)$$

This equation was noticed in the little tub. However, this equation fails to predict speed over a vast area. This is accomplished by considering the qualities of waves. They are used to determine the wavelength of waves on a vast scale.

$$\lambda = height * C/2 * depth \quad (3)$$

*Height re*presents height of wave and *C* shows wave speed. Height *can be calculated by*, Equ (4).

$$\mathbf{Height} = ½ * depth / \sqrt[4]{8 * \pi * depth/L} \quad (4)$$

L and depth indicate depth of water and wavelength to compute L.

$$L = L_o \sqrt{\tan h(2 * \pi * depth/L_o)} \quad (5)$$

L_o is wave speed at Height

$$L_o = C^2 * 2 * \pi/gf \quad (6)$$

$$C = \sqrt{gf * depth} \quad (7)$$

$$L_o = (\sqrt{g}f)^2 * 2 * \pi / gf \quad (8)$$

$$L_o = gf * depth * 2 * \pi / gf \quad (9)$$

$$L_o = 2 * \pi * depth \quad (10)$$

We put value L_o *in Eq(5)*

$$L = 2 * \pi * depth \sqrt{\tan h(2 * \pi * depth/2 * \pi * depth)} \quad (11)$$

$$L = 2 * \pi * depth \sqrt{\tan h(1)} \quad (12)$$

$$L = 2 * \pi * depth \sqrt{0.76} \quad (13)$$

$$L = 2 * \pi * depth * 0.87 \quad (14)$$

$$L = 1.74 * \pi * depth \quad (15)$$

Placing value of L in eq (4)

$$\mathbf{Height} = ½ * depth / \sqrt[4]{8 * \pi * depth/1.74 * \pi * depth} \quad (16)$$

$$\mathbf{Height} = ½ * depth / \sqrt[4]{4.5} \quad (17)$$

$$\mathbf{Height} = ½ * depth / 1.45 \quad (18)$$

$$\mathbf{Height} = 0.34 * depth \quad (19)$$

Now w put Height and C into Eq(3) to compute λ.

$$\lambda = 0.34 * depth * \sqrt{gf * depth}/2 * depth \quad (20)$$

$$\lambda = 0.17 * \sqrt{gf * depth} \quad (21)$$

Sink nodes can use Algorithm1 to relocate from their predefined to next position when nodes are deployed. Each node determines its approximate X axis location with the help of sink nodes, whilst the Y axis of each node is measured by the depth of water in an underwater environment. Here, gf represents the gravitational force, pre_time represents the previous time when the topology was changed, r and z represent the node's x and y axes, shows the wavelength, speed demonstrates the water speed at the current depth level, and time calculates the time of last change with regard to the present time, which allows us to measure the actual position of a node.

Since waves flow in a circular pattern and a circle encompasses the range 0 to 360. The origin of each quadrant is the central point of each circle, and it encompasses all four quadrants; thus, speed is divided by four. This approach assists us in determining the approximate change in node movement, either forward or backward. Utilizing stage 11 of Algorithm1, we determine a specific node movement after computing wave speed at the present desired density and duration.

3.2. Two Nodes Reliable Model (2n-Rm)

2N-RM is introduced for building dependable linkages, with three major elements considered: distance, Expected Transmission Count (ETX), as well as remaining energy.

3.2.1. Distance

Routing protocols determine the range limit for each sensor node. Sensor nodes in the AODV, DSDV, and DSR protocols have a default range restriction of 250 m, but nodes in the VBF and DBR protocols have a range limit of 100 m. As a result, the destination or intermediary node must be located within this range in order to receive data from the source node. The range limit of nodes in TBRL is set to 70 m, and the Euclidean distance in between the origin and the next forwarder is estimated.

$$\textbf{Distance}=\sqrt{(\boldsymbol{A2}-\boldsymbol{A1})^2}+\ (\boldsymbol{B2}-\boldsymbol{B1})^2 \qquad (22)$$

$$70>\text{Distance}>0$$

A_2, A_1, B_2, and B_1 show the position of n2 X, n1 X, n2 Y, and n1 Y, correspondingly.

The dependability of the connections is proportional to the difference between nodes. Less distance implies more reliability, but more distance equals worse reliability. The ge limit is defined to 70 m and calculates the Euclidean distance among source to distance is going to be in range of (0 to 70) by maintain the ge limit is set to 70 m and calculates the Euclidean distance among the source and the distance must be greater than 0 and less than 70 m By keeping the ge limit to 70 m and calculates the distance among the source and the credible connection. The dependable link must meet the specified criteria. The ge limit is 70 m and generates the Euclidean distance between the source and the succeeding link which typically indicates identifying a resource with good high precision and recall and getting an accurate depiction of the source in a reasonable timeframe.

i.e the limit is set to 70 m, and the algorithm calculates Euclidean distance with a suitably low latency and bit error rate. The parent is picked among neighbors based on link estimate methods and distance to place the dependable links in routing tables rather than those supported by hop count. The metrics employed investigate cross-layer information to improve dependability, and the ties among neighbors are examined in an extremely probable and accommodating way to assess perhaps not yet selected nodes with quick exploring and silent link observation techniques.

Algorithm 1 **Dynamic Topology Discovery**

Input: Every node from source to sinks
Output: Compute every node location

Initialization:
1: $gf = 9.81$ (Gravity is same water and air)
2: $pre\_time = 0$ (previous time of node)
3: **for** $k = 1$ *to all nodes* **do**
4: $r = LocP[k]$ (Location Packet)
5: $z = Node\_depth[k]$
6: $\lambda = 0.17 * \sqrt{gz}$
7: $speed = ((\sqrt{gf * \lambda})/(2 * \pi)) * tanh(2 * \pi * z/\lambda))$
8: $r1 = speed/4$
9: $t = c\_time - pre\_time$
10: $r2 = t * r1$
11: $node[k]\ ((r \pm r2), z)$
12: $pre\_time = c\_time$

13: *End for*

3.2.2. Expected Transmission Count

ETX is a key metric for assessing link reliability. It measures the likelihood that a packet will be delivered successfully and acknowledged via a link. ETX is calculated using the equation shown below:

ETX= 1/Sra *Acr (23)

The 70 m distance limit and the Euclidean distance between source and reflect the payload sending ratio (Sra) and packet acknowledgment ratio (Acr), respectively. The delivery ratio, which is a key factor in the throughput of the network, is what determines ETX. As well as choosing the best path for the payload, it calculates the path loss ratio.

3.2.3 Residual Energy

Calculating the sensor node's power status is an additional factor. Each of the network participants needs to be active and have enough energy to send and receive datagram. All active nodes must be part of a dependable network from origin to destination.

3.2.4 Reliable Paths Establishing

All of the chosen nodes turn into source nodes and begin looking for additional trustworthy nodes when 2N-RM is used. As a result, numerous trustworthy receivers are identified, and the process repeats until the sink nodes are approached. Figure4 shows a single source's consistent nodes identification to many sinks.

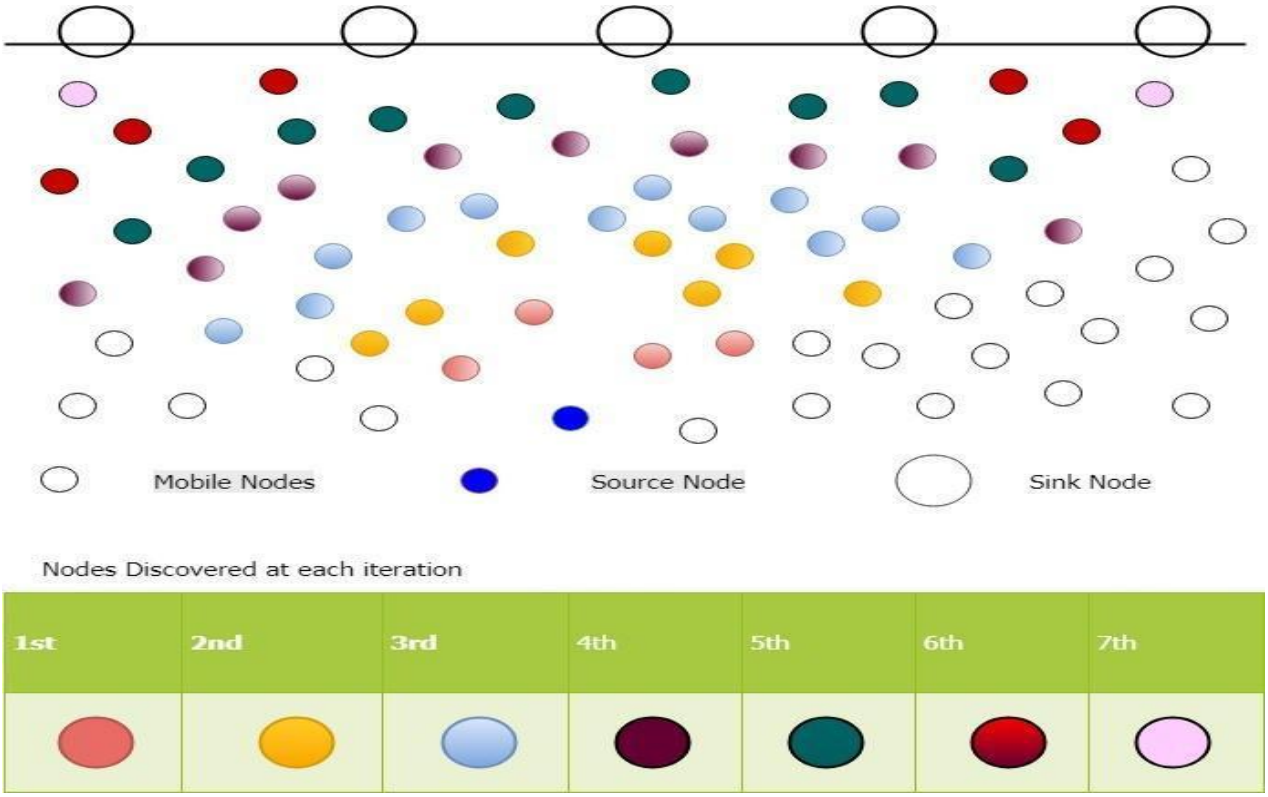

Figure 4. Reliable Nodes Discovery

Multiple pathways are constructed from source to destination node nodes when the dependable nodes have been found. We created a tree topology using our dependable nodes. In this topology, the original source node turns into the root node, while every sink acts like a leaf node. Child nodes are multiple intermediary nodes that form a path from the root to the leaf nodes. Tree structure of proficient routes is shown in Figure5. Every stage demonstrates that there is never a round or network and that each child has a single parent. A node chooses a parent based on first come, first serve when it receives numerous requests. Closer nodes have less power usage, bandwidth, latency, and reliability in their information transmission thanks to acoustic communication.

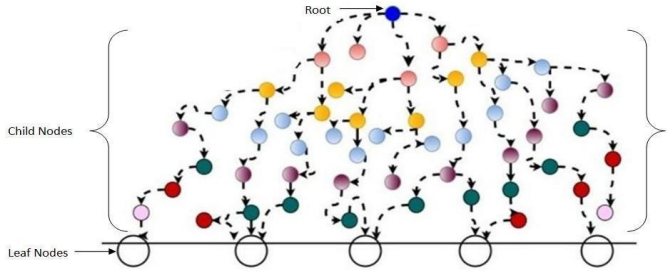

Figure 5. Tree Topology of Establishing Paths.

3.2.5 Selection Process of Reliable Link

A greeting packet is sent by the source host to its neighbors in 2N-RM. The single field in the hello packet format is the node id. Nodes transmit an acknowledgment to the source host after receiving a greeting packet. Remaining energy, position, and recipient node id make up the acknowledgement packet format. The source node then determines the physical distance and evaluates its position in relation to other nodes. Nodes with a higher Y axis whose distance from the queue is greater than 70 m will be eliminated. The sender and the chosen nodes have established a link, and the consistency of each node is assessed using the ETX value by sending 10 hello messages after a predetermined period of time. Each link's outcome is placed in a queue after the calculation of Sr and Ar. The output is saved in ascending order for all results. If a link's value is closer to 1, it will be chosen as the most consistent path.

Such a sorting method shortens the time needed by 2N-RM to choose additional nodes in the case of a diseased node or a node with reduced residual energy. We identify the best path with regard to the participation of the most nodes by taking advantage of tree features. The Iterative Depth First Search (IDFS) algorithm is employed for this purpose. The ideal path is presented to us by IDFS, which sorts the paths. Data packets will be forwarded in the direction of the sink node after choosing the best route. Due to the severe underwater environment, a node with a lower distance than the others will be chosen even when all nodes within the predetermined limit have about the same ETX value. (see Figure6).

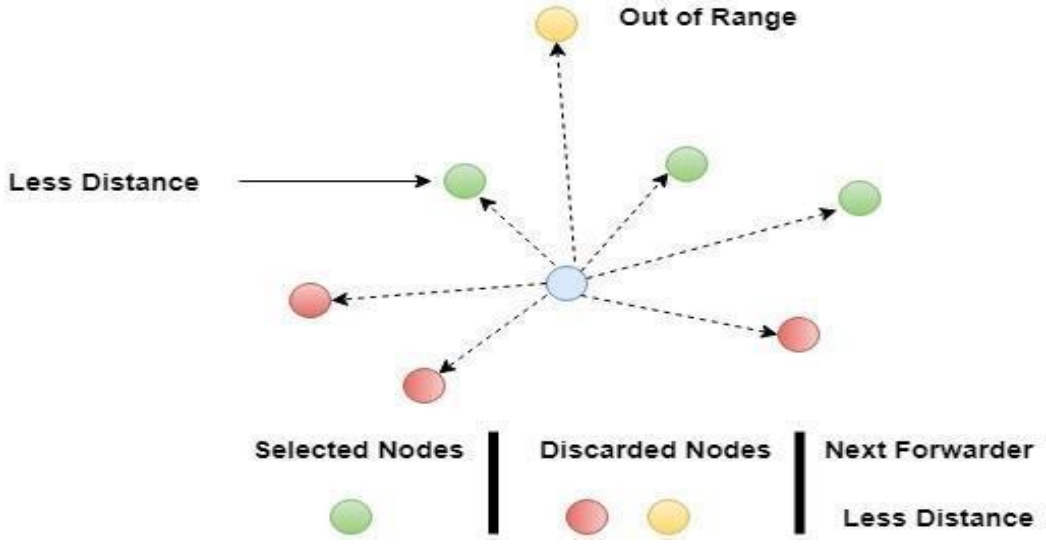

Figure 6. Next Forwarder Selection.

3.3 *Dynamic Topology Discovery of Existing Paths*

For TBRL to check the impacted paths using dynamic topology, Algorithm2 is suggested in this part. At first, all of the routes leading from a source to various sinks are accepted as input parameters. These pathways were all the result of various nodes. Each path's nodes have been retrieved and saved in an array at step 2. Each node's performance has been determined after several nodes have been inserted inside the array. The wavelength of the wave indicated by Equation (21), "lambda," and the depth of the node are all factors in the step where speed is computed. Each node is aware of its location and depth level since TBRL uses a positioned-based routing method. Step 6 involves saving the updated position of the node in a different collection. All fresh pathways have been pulled out and travelled after the outer circle has been completed. These paths are then further assigned to the source node. Next, IDFS is invoked, and it chooses the path that has the greatest number of various nodes between the source and the destination nodes.

Algorithm 2 Dynamic Topology Discovery of Existing Paths

Input: Eery Paths (source to sink) fetched through IDFS
Output: topology effected paths

***Initialization*:**

1. for j= 1 *to All Paths* do
2. P_nodes[]=j (nodes which are making path)
3. For k=0 to p_nodes do
4. $speed = \sqrt{(((gf * \lambda)/(2 * \pi)) * tanh(2 * \pi * depth_j/\lambda))}$
5. $mov = speed/4$
6. $nod_{jj}=nod_k((Z \pm mov),X)$
7. $nod_k=nod_{jj}$
8. $n\_P\_nodes[\,] = node_k$
9. *end for*
10. $Path_l = n\_P\_nodes[\,]$
11. end for
12. return $Paths_j$
13. for u=1 to Paths do (received path from phase 12 will be accommodated in given below steps)
14. Call IDFS(u)
15. Compare Number of Nodes Participating
16. Select path having higher nodes participation
17. end for

---

4 Mathematical Model

The talk that follows looks at two quantitative ways to estimating energy consumption and time slots. This section specifies the time window that a sender must have available to send packets of data to a sink node. to s is utilized as a set time period in the first iteration. Before collecting a greeting packet, the source node transmits one and waited for other nodes to recognize it. Because numerous receivers react throughout that time period, the aggregate time is determined. This average time will be used for the upcoming iteration's schedule assignment.

$$T_1 = \sum NuRT / \_NNode \qquad (24)$$

where, ∑ NuRT is the sum of all node response times, and NNode is the number of nodes that respond. Similarly, in the following cycle, numerous nodes become source nodes, resulting in a dependable network. There have been two summation signs used in Equations (25)-(28): receivers' response time sum is indicated by first summation whereas the second one assigns limit from 1 to n, here n shows the total number of sender nodes mentioned in the preceding iteration and the outer summation sign acts as a loop.

$$T_2 = \sum_{j=1}^{n} \sum NuRT_j / \_NNode_j \qquad (25)$$

Mean time needed y source node for n iterations is computed as:

$$T_n = \sum_{j=1}^{n} \sum NuRT_j / \_NNode_j \quad (26)$$

Sum for mean time is:

$$t_{tt}=t1+t2+t3.....t_n \quad (27)$$

$$t_{tt}= \sum NuRT / \_NNode + \sum_{j=1}^{n} \sum NuRT_j / \_NNode_j + ... \sum_{j=1}^{n} \sum NuRT_j / \_NNode_j \quad (28)$$

b represent total number of nodes in network

$$t_{tt}= \sum NuRT / \_NNode + \sum_{r=1}^{b} [\sum_{j=1}^{n} \sum NuRT_j / \_NNode_j] \quad (29)$$

The outcomes of t1 can be determined using the following phrase, which is the total of average node response time. As a result, Equation calculates the average time taken by a sender to reach any sink node (30).

$$t_{tt}=\sum_{r=1}^{b} [\sum_{j=1}^{n} \sum NuRT_j / \_NNode_j] \quad (30)$$

4.1 Energy Consumption

We considered the variables included in Table 2 to determine our model's energy consumption.

Table 2. Parameters for Energy Consumption.

HEPS	Hello Packet Sending
HEPR	Hello Packet Receiving
HPRAC	Hello Packet Receiver Acknowledgment
DAPE	Data Packet Energy Consumption
N	Number of Iterations
TEC	Total Energy Consumed
E_i	Energy Consumed at ith
Iteration TDP	Total Data Packet

4.1.1 Energy Consumed by HEPS, HEPR and HPRAC

Due to HPR's dual receiving energy usage, it is done twice as often as HPS and HPRA. The HPS and HPR energy that is used up throughout each loop is expressed as follows:

$$E_1 = HEPS + 2HEPR + HPRAC \quad (31)$$

for N number of nodes energy consumption is:

$$E_N = N(HEPS + 2HEPR + HPRAC) \quad (32)$$

4.1.2 Energy Consumed by DAPE

Data packets are sent to a chosen node that is trustworthy in terms of the distance; as a result, energy consumption by DAPE is computed as:

$$E_1=DAPE \quad (33)$$

For TDA and N consumption of energy is computed as:

$$E_N = N(TD * DAPE) \quad (34)$$

By combining both we get:

$$\text{TE} = N(HEPS + 2HEPR + HPRAC) + N(TDP * DAPE) \quad (35)$$

Energy usage for HRPAC and HEPS is the same, with HEPR using slightly more energy (1/5) than HEPS. So equ (35) becomes:

$$\text{TE} = \text{N}(\text{TDP} * \text{DAPE}) + \text{N}(\text{HEPS} + \frac{2\text{HEPS}}{5} + \text{HEPS}) \quad (36)$$

$$TE = N^{*}(TDP * DAPE) + N(2.4 * HEPS) \quad (37)$$

$$TE = N(TDP * DAPE) + N(2.4 * HEPS) \quad (38)$$

$$TE = N((TDP * DAPE) + 2.4 * HEPS) \quad (39)$$

Ship turbulence, sea currents, wind velocity, biotic noises, etc. all have an impact on energy. SNR is consequently included in the calculation of total energy. The equation that follows is used to compute SNR.

$$TE = N((TDP * DAPE) + 2.4 * HEPS) + SNR \quad (40)$$

$$SNR = SLevel - TransLoss - NLevel + DIndex \quad (41)$$

here SLevel is the source node's goal noise level, TransLoss is the transmission loss, NLevel is the receiver's and the atmosphere's noise level, and DIndex is the directive index. NLevel, DIndex, and SNR values are extracted from [34]. Table3 lists their results for deep water. The following equation gives the deep sea TransLoss.

$$TransLoss = 20logd + \alpha * d * 10^{-3} \quad (42)$$

Table 3. Physical layer model.

Parameter	Value
NLevel	70 dB
DIndex	3 dB
SNR	20 dB

TransLoss is inversely correlated with frequency dependent absorption and distance dependent attenuation. Thorp's expression uses the following equation to calculate for frequencies greater than a few hundred Hertz

$$\alpha = \frac{0.1 * f^2}{(1 + f)^2} + \frac{40 * f^2}{4100 + f^2} + 2.75 * 10^{-4} f^2 + 0.003 \quad (43)$$

$$\alpha = \frac{0.11 * f^2}{(1 + f)^2} + 0.011 * f^2 + 0.002 \quad (44)$$

where f is expressed in kHz and alpha is expressed in dB/km. The following formula can be used to compute SL, which is directly connected to signal strength at a distance of 1 m from the signal's source.

$$SL = 10\log \frac{I_T}{1vP_a} \quad \textbf{(45)}$$

Transmission power P_t for sources from the deep sea.(d), which is in $Watts/m2$, is calculated as:

$$P_T(d) = 4\pi * (1m)^2 * I_T \quad \textbf{(46)}$$

The overall energy consumption of a network with N nodes at various depths and TD is determined by Equation (40).

5 Simulation and Results

Through simulations, we assessed the effectiveness of the TBRL routing protocol in this section. We paired the 2N-RM with the TBRL in order to emphasize the TBRL's exceptional features, and we compared the TBRL's efficiency to that of DBR and the Reliable Energy-efficient Routing Protocol (R-ERP2R). In the following section, the simulations' environment and outcomes are described.

5.1 *Simulation Setting*

To evaluate TBRL, NS-2 with the Aquasim program is utilized. In a space of 1000 m2 x 1000 m2, 500 mobile nodes were randomly placed inside the water, while numerous sink nodes were positioned on the water's surface. The sink nodes have radio and audio communication capabilities. While the rest of the nodes in the water can move between 1 and 4 m/s, sink nodes are thought of as static throughout the simulation environment. Node movement in the diagonal and vertical directions is disregarded. For the simulation environment, only horizontal node movement is considered. TBRL is evaluated against several sets of nodes. Two source nodes that have been installed on the seafloor. The size of each data packet is set at 1000 bytes. Each source node produces traffic with a fixed bit rate. The average value of 50 simulation runs for each node dataset is used to calculate the experimental results. Table4 illustrates the simulation parameters offered to TBRL as well.

5.2 Results and Discussion

Figures7–15 display the outcomes of the simulation. The simulation tool is NS-2 AquaSim, an NS-2 simulator plugin that was created specifically for aquatic environments. The simulation parameters are provided in Table 4. The simulation results are explained in two phases: in the first phase, all of the trustworthy links between the nodes are established at various depth levels, and these links are assessed in terms of throughput, energy consumption, packet delivery ratio, and time. Additionally, the PDR of its reliability model is contrasted with that of the 3H-RM and the 2H-ACK. With regard to end-to-end latency, PDR, and EC of the network, TBRL compares its performance to that of DBR and R-ERP2R in the second phase.

Table 4. Simulation Setting.

Parameter	Value
Area	1000 × 1000 m^2
Nodes Data Set	50, 100, 150, ..., 500
Sink Nodes	5
Data Packet Size	1000 Bytes
Communication Medium	Wireless
Wireless Channel	Radio and Acoustic
Radio Speed	3×10^8 m/s
Acoustic Speed	1500 m/s
Transmission Range	70 m
Frequency	15 KHz
Energy	Energy Model
Initial Energy	1000 J

Transmission Power	0.5 W
Receiving Power	0.1 W
Idle Power	0.008 W
Sleeping Power	0.01
Physical Layer	UnderwaterPhy
Mac Layer	UnderwaterMac
Antenna	OmniAntenna
Nodes Mobility	Random
Network Topology	2D

5.2.1 Time

Making a path across various nodes in the dataset to reach the sink nodes takes time. The longest possible time is needed to establish a path from the source to the destination node for the tiny selection of nodes. Because it is easier to choose the next node when there are more nodes, TBRL needs less time. Only the path with the shortest forwarding time is considered by TBRL when choosing a path in a multiple path environment. Figure7 compares several routes in terms of time.

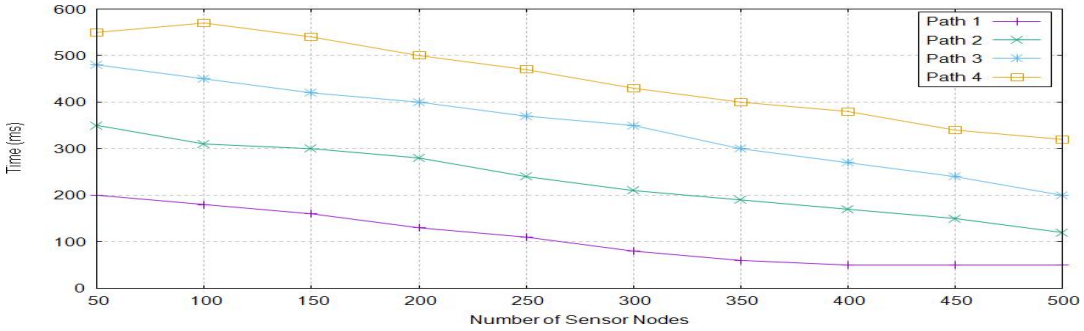

Figure 7. Reliable Paths Creation Time in TBRL.

5.2.2 Packet Delivery Ratio

The packet delivery ratio indicates a high success rate. It is determined by dividing the total packets transmitted from all source nodes by the total packets received at all destination node. The delivery ratio of TBRL approximately reaches 99 percent when all nodes are present in the network, as illustrated in Figure 8, however the transmission range of data is poor when there are few nodes. Less nodes indicate a greater distance among them, increasing the likelihood of packets being dropped, which is a major factor in these results.

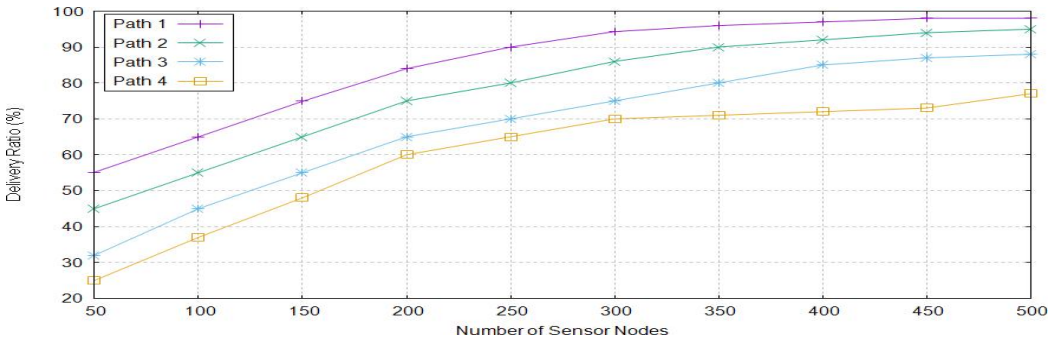

Figure 8. Packet Delivery Ratio of Different Paths in TBRL.

5.2.3 Energy Consumption

Energy consumption of nodes refers to how much energy nodes use over the course of their existence. The total power consumed by their packet sending, packet receiving, sleeping, and idle states. Through the energy model, these variables are initialized. Additionally, the previous section discussed the mathematical model of energy use. The value of energy consumption is calculated using equation (47).

$$TE = TDP * DAPE + 2.4 * HEPS + SNR \quad (47)$$

The abbreviations TE, TDP, DAPE, HEPS, and SNR stand for total energy consumption, total data packets, datagram energy, sending hello packets, and SNR. A network is created for various node configurations, and Section4.1 analyses how much energy each node consumes. The network chooses path1 because nodes keep path1 alive and active for a longer period of time and with less power consumption. The energy use of pathways is depicted in Figure9.

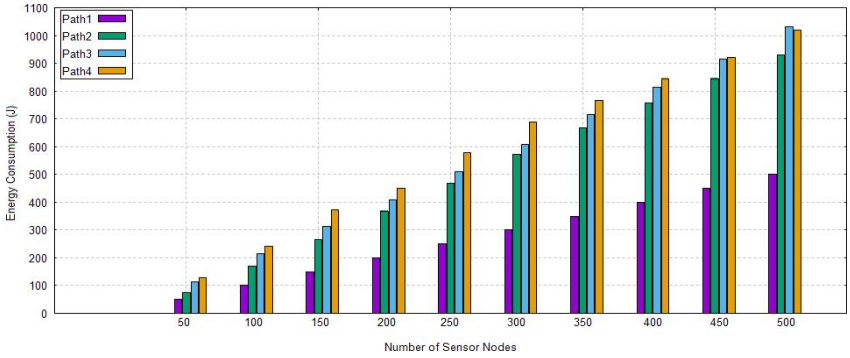

Figure 9. Energy Consumption of Different Paths in TBRL.

5.2.4 Throughput

Successful packet delivery to the sink node is the definition of throughput. Without knowing how many packets were sent overall, it just considers the ones that are received. In TBRL, the throughput values for various pathways vary.Figure10 illustrates that path 2 and 4 have higher throughput than path 1 and 2.

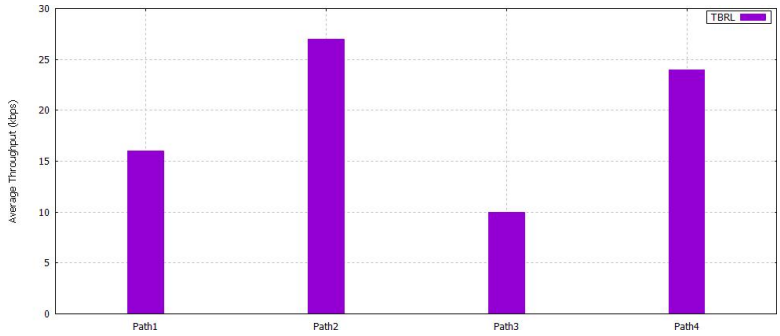

Figure 10. Throughput among Different Paths in TBRL.

5.2.5 Transmission Loss

Transmission loss is measured using Equation (48).

$$TransLoss = 20 log d + \alpha * d * 10^{-3} \quad (48)$$

When the transmission level (TL) is represented in decibels (dB), the sender-to-receiver distance (d) is given in meters (meters), and the absorption (dB/km) is computed. According to equation (48), attenuation due to distance and absorption due to frequency are the main causes of transmission loss. The receiver's performance suffers significantly from transmission loss. As attenuation loss and transmission range rise, it does as well. Acoustic systems can function between 10 and 15 kHz in terms of frequency. Even though system's overall communication bandwidth is very small (5 kHz), it is wideband in the view that it does not have an insignificant impact on the central frequency. Since the greatest distance between two functional nodes in TBRL is 70 m, we chose d to be 70 m and calculated transmission loss for various frequencies, as shown in Figure11.

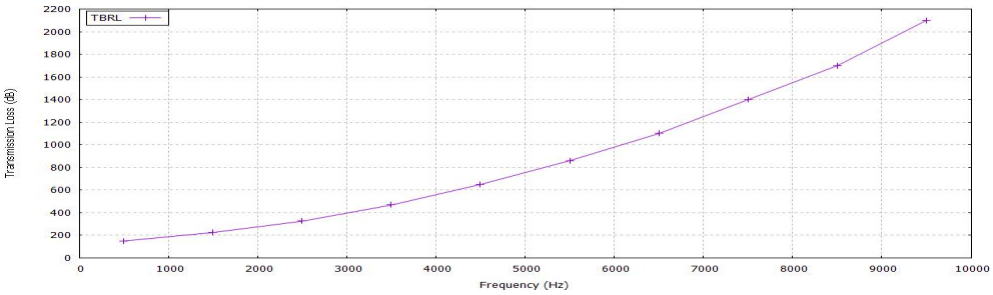

Figure 11. Maximum Transmission Loss in TBRL

5.3 *Packet Delivery Ratio of 2n-Rm*

When the phase margin is less than 3 and the datagram has arrived at the sink node, 3H-RM does not offer any mechanisms for the acknowledgment phase. Similar to this, when the second node in 2H-ACK turns into a sink, it is forced to accept acknowledgment from other receivers and send it to the source node. The source node will flood the data packet again to the next node after waiting 60 seconds for the acknowledgment. As a result, a cycle that will raise power consumption, redundant data at the end nodes, and network end-to-end delay begins between both the sink and origin nodes. Two node reliability models are part of the 2N-RM. Compared to these two models, it has a lighter greeting payload and acknowledgment packet format. Because to the one-to-one link, there is no chance of a duplicate data packet occurring when data reaches the sink node.

Packet Delivery Ratio of 2n-Rm

Figure12 displays the PDR for each of these models. As the number of nodes grows, PDR increases. Because they use the same approach, and more than two nodes participate in the dependability test, 3H-RM and 2H-ACK have approximately the same PDR. However, in 2N-RM, only two nodes guarantee dependability by taking the ETX value into account. Therefore, comparing to 3H-RM and 2H-ACK, 2N-RM has a greater PDR.

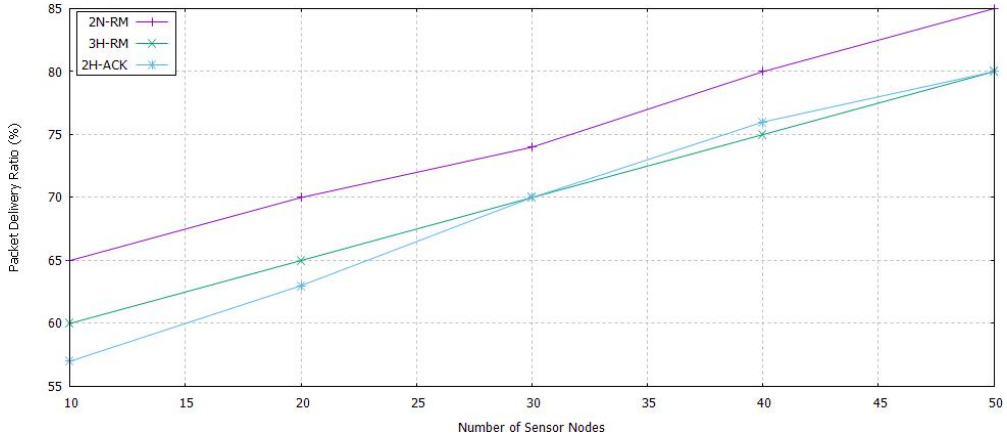

Figure 12. Packet Delivery Ratio of 2N-RM, 3H-RM, and 2H-ACK.

5.4 *Performance Analysis of Tbrl with Dbr and R-ERP^{2}R*

We used the DBR protocol and R-ERP2R to compare with our suggested routing protocol. The next node is located using DBR using a greedy technique versus nodes depth. The next routing has been chosen, and it is a node with less depth than the other nodes. It is a good choice for controlling dynamic topology because of its greedy nature. R-ERP2R chooses the subsequent node using a greedy strategy, but it also takes the subsequent node's residual energy value and physical distance into account. Additionally, it guarantees a link's caliber. As a result, we compared our findings to DBR and R-ERP2R. The identical node datasets and simulation parameters are applied to them, and the results in terms of delivery ratio, time, and energy usage are gathered.

5.4.1 End to End Delay

Figure13 compares the time to transfer datagram to the time to build a path from source to destination node. DBR takes up more time than TBRL in some simulation results, but it takes up less time than TBRL in other findings. Due to DBR's opportunistic strategy, this has occurred. DBR can occasionally produce successful outcomes. Values have been assigned to the TBRL after averaging the positive and negative results. R-ERP2R does not specify a maximum range for physical distance; instead, it uses a greedy strategy to select the next path and only creates one for data transmission. The physical distance is predetermined in TBRL, and it considers a variety of potential routes from source to sink. It then sorts the routes and selects the one with the least amount of delay.

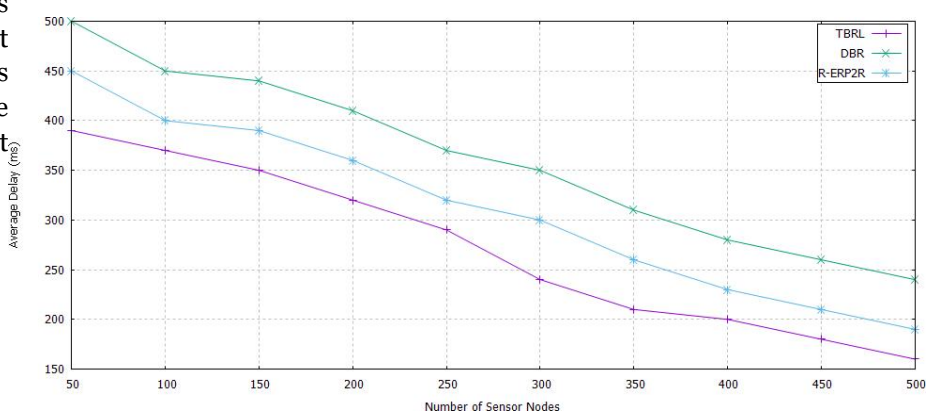

Figure 13. End to End Delay of TBRL, Depth Based Routing (DBR), and Reliable Energy-efficient Routing Protocol (R-ERP^2R).

5.4.2 Packet Delivery Ratio

Figure14 displays the delivery ratio of the TBRL in comparison to the DBR and R-ERP2R. In contrast to TBRL, which already has trustworthy nodes and paths identified and filtered using IDFS, both protocols store data packets until the finest next node is determined. As a result, the TBRL delivery ratio is high.

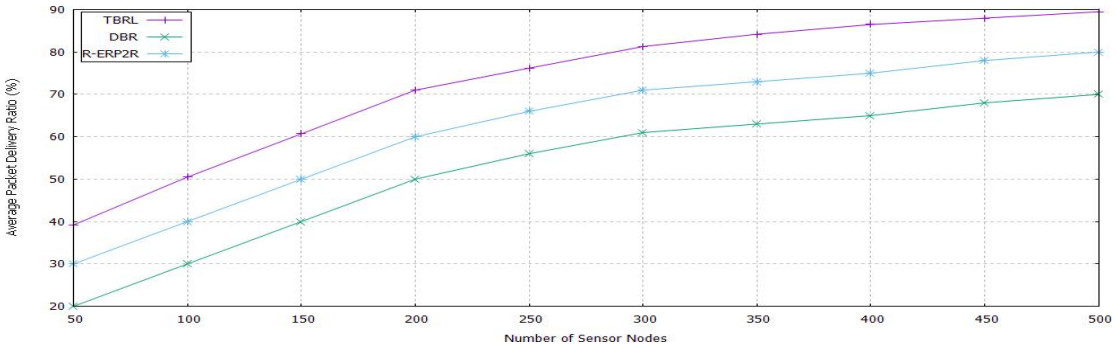

Figure 14. Packet Delivery Ratio of TBRL, DBR and R-ERP^2R.

5.4.3 Energy Consumption

To determine which receiving node is the finest between them, DBR and R-ERP2R evaluate the nodes' depth, distance, remaining energy, and link quality. The amusement of several receivers results in wasteful energy consumption in the form of datagram receiving, waking up dormant nodes, and changing the power state from idle to active. As shown in Figure15_46r0c02, the energy consumption of TBRL is lower than that of DBR and R-ERP2R since multiple receivers could not be supported.

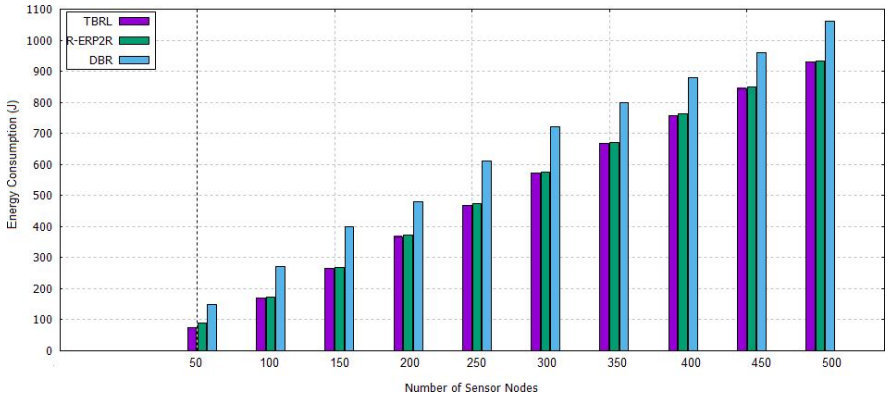

Figure 15. Energy Consumption of TBRL, DBR and R-ERP^2R.

5 Conclusions

Building dependable links is a crucial necessity for I-UWSN and smart environments. As a result, we have looked into the metrics that are impacted by weak link reliability. Dynamic topology is a key contributor to the weak link dependability, and its effects can be seen in the metrics of transmission loss, packet delivery ratio, network longevity, and throughput. Because to the water's constant flow, dynamic topology develops. As a result, it is impossible to create a trustworthy link for a long period. Because short time reliability can be attained, we have presented TBRL for the dynamic topology routing protocol in this work. Using a topology discovery algorithm, TBRL first determines the general location of each sensor node. Only nodes depth is taken into consideration as an input parameter for determining node position. Then, using each subsequent forwarder's distance, ETX, and residual energy level, TBRL calculates the link reliability of each one. Up until the sink is reached, TBRL keeps establishing a solid bond. Multiple trustworthy routes are constructed in this manner from sources to sinks. The most reliable path has been chosen based on the highest number of nodes participating. In order to determine the time interval, the average time calculation is considered. The two nodes reliability model is then given this average time to select the subsequent forwarder. With DBR and R-ERP2R, we assessed how well our suggested protocols performed in terms of packet delivery rate, end to end delay, throughput, and network energy usage. We also compared the packet delivery ratio of 2N-RM to that of 2H-ACK and 3H-RM. The simulation results demonstrate that TBRL outperforms state-of-the-art methods. The findings show that TBRL is a superior protocol for underwater sensor communication and sensor monitoring, supporting the goal of smart cities. In the future, we'll employ machine learning methods to select paths more efficiently.

Author Contributions: T.A. and A.S. conceptualised the research and developed the approach (Ahmad Shaf). T.A., A.S. (Ahmad Shaf), and M.A. perform the technical work and simulations (Muhammad Aamir). M.A. (Muhammad Awais) and A.S. performed the technical evaluation and adjustments (Ahmad Shaf). A.S.A., A.S. (Ahthasham Sajid), and M.I. manage the project's administration and provide general technical support. Finally, A.S. (Ahmad Shaf) and M.A. provided answers to the reviewers' questions (Muhammad Awais). The manuscript's published form was approved by all authors after they had read it.

Funding: The Saudi Arabian Ministry of Education's Study and Development Office provided funding for this research project. In collaboration with Najran University Saudi Arabia, the Saudi Ministry of Education provided post-doctoral funding for the APC.

Acknowledgments: The Saudi Arabian Ministry of Education's Research and Development Office, in collaboration with Najran University, provided the authors with support in the form of a post-doctoral fellowship, which they gratefully welcome.

Conflicts of Interest: There is no conflict of interest.

References

1. Awais, M.; Javaid, N.; Rehman, A.; Qasim, U.; Alhussein, M.; Aurangzeb, K. Towards Void Hole Alleviation by Exploiting the Energy Efficient Path and by Providing the Interference-Free Proactive Routing Protocols in IoT Enabled Underwater WSNs. *Sensors* **2019**, *19*, 1313. [CrossRef]
2. Kim, H.-W.; Cho, H.-S. SOUNET: Self-organized underwater wireless sensor network. *Sensors* **2017**, *17*, 0283. [CrossRef]
3. Khalid, M.; Ullah, Z.; Ahmad, N.; Arshad, M.; Jan B.; Cao, Y.; Adnan, A. A Survey of Routing Issues and Associated Protocols in Underwater Wireless Sensor Networks. *J. Sens.* **2017**, *2017*, 17. [CrossRef]
4. Diamant, R.; Francescon, R.; Zorzi, M. Topology-Efficient Discovery: A Topology Discovery Algorithm for Underwater Acoustic Networks. *IEEE J. Ocean. Eng.* **2017**, *43*, 1200–1214. [CrossRef]
5. Felemban, E.; Shaikh, F.K.; Qureshi, U.M.; Sheikh, A.A.; Qaisar, S.B. Underwater sensor network applications: A comprehensive survey. *Int. J. Distrib. Sens. Netw.* **2015**, *11*, 896832. [CrossRef]
6. Li, N.; Martínez, J.-F.; Chaus, J.M.M.; Eckert, M. A survey on underwater acoustic sensor network routing protocols. *Sensors* **2016**, *16*, 414. [CrossRef]
7. Chen, B.; Pompili, D. Reliable geocasting for random-access underwater acoustic sensor networks. *Ad Hoc Netw.* **2014**, *21*, 134–146. [CrossRef]
8. Diamant, R.; Bucris, Y.; Feuer, A. An efficient method to measure reliability of underwater acoustic communication links. *J. Ocean. Eng. Sci.* **2016**, *1*, 129–134. [CrossRef]
9. Prakash, T.S.; Raja, K.; Venugopal, K.; Iyengar, S.; Patnaik, L. Link-Reliability Based Two-Hop Routing for Wireless Sensor Networks. *arXiv* **2014**, arXiv:1403.0001.
10. Vigita, S.R.; Julie, G. Reliable Link-Based Routing Protocol for Highly Dynamic Mobile Adhoc Networks. *arXiv* **2014**, arXiv:1402.1819.
11. Li, N.; Cürüklü, B.; Bastos, J.; Sucasas, V.; Fernandez, J.A.S.; Rodriguez, J. A Probabilistic and Highly Efficient Topology Control Algorithm for Underwater Cooperating AUV Networks. *Sensors* **2017**, *17*, 1022. [CrossRef] [PubMed]
12. Kafi, M.A.; Othman, J.B.; Badache, N. A Survey on Reliability Protocols in Wireless Sensor Networks. *ACM Comput. Surv. (CSUR)* **2017**, *50*, 31. [CrossRef]
13. Ayaz, M.; Abdullah, A. Hop-by-hop dynamic addressing based (H2-DAB) routing protocol for underwater wireless sensor networks. In Proceedings of the 2009 International Conference on Information and Multimedia Technology, Jeju Island, Korea, 16–18 December 2009; IEEE: Piscataway, NJ, USA, 2009; pp. 436–441.
14. Geethu, K.; Babu, A. Erasure Codes Based Adaptive Multi-hop Reliable Data Transfer for Underwater Acoustic Sensor Networks. *Wirel. Pers. Commun.* **2017**, *94*, 579–604. [CrossRef]
15. Patil, S.; Gothawal, D.B.; Wagh, S.J. A cross-layer topology control with clustering and routing for energy efficient wireless sensor networks. In Proceedings of the 2014 International Conference on Green Computing Communication and Electrical Engineering (ICGCCEE), Coimbatore, India, 6–8 March 2014; IEEE: Piscataway, NJ, USA, 2014; pp. 1–5.
16. Liu, L.; Du, J.; Liu, Y. Topology control for diverse coverage in underwater wireless sensor networks. *ACM Trans. Auton. Adapt. Syst.* **2016**, *11*, 16. [CrossRef]
17. Basagni, S.; Petrioli, C.; Petroccia, R.; Spaccini, D. CARP: A channel-aware routing protocol for underwater acoustic wireless networks. *Ad Hoc Netw.* **2015**, *34*, 92–104. [CrossRef]
18. Jha, D.K.; Wettergren, T.A.; Ray, A.; Mukherjee, K. Topology optimisation for energy management in underwater sensor networks. *Int. J. Control* **2015**, *88*, 1775–1788. [CrossRef]
19. Chen, J.; Wu, X.; Chen, G. REBAR: A reliable and energy balanced routing algorithm for UWSNs. In *Grid and Cooperative Computing, Proceedings of the 2008 Seventh International Conference on Grid and Cooperative Computing, Shenzhen, China, 24–26 October 2008*; IEEE: Piscataway, NJ, USA, 2008; pp. 349–355.
20. Ghoreyshi, S.M.; Shahrabi, A.; Boutaleb, T. An opportunistic void avoidance routing protocol for underwater sensor networks. In *Advanced Information Networking and Applications (AINA), Proceedings of the 2016 IEEE 30th International Conference on Advanced Information Networking and Applications (AINA), Crans-Montana, Switzerland, 23–25 March 2016*; IEEE: Piscataway, NJ, USA, 2014; pp. 316–323.
21. Sher, A.; Khan, A.; Javaid, N.; Ahmed, S.H.; Aalsalem, M.Y.; Khan, W.Z. Void Hole Avoidance for Reliable Data Delivery in IoT Enabled Underwater Wireless Sensor Networks. *Sensors* **2018**, *18*, 3271. [CrossRef]
22. Coutinho, R.W.; Boukerche, A.; Vieira, L.F.; Loureiro, A.A. GEDAR: geographic and opportunistic routing

protocol with depth adjustment for mobile underwater sensor networks. In Proceedings of the 2014 IEEE International Conference on Communications (ICC), Sydney, NSW, Australia, 10–14 June 2014; IEEE: Piscataway, NJ, USA, 2014; pp. 251–256.
23. Coutinho, R.W.; Vieira, L.F.; Loureiro, A.A. DCR: Depth-Controlled routing protocol for underwater sensor networks. In Proceedings of the 2013 IEEE Symposium on Computers and Communications (ISCC), Split, Croatia, 7–10 July 2013; IEEE: Piscataway, NJ, USA, 2013; pp. 000453–000458.
24. Zhao, W.; Tang, Z.; Yang, Y.; Wang, L.; Lan, S. Cooperative search and rescue with artificial fishes based on fish-swarm algorithm for underwater wireless sensor networks. *Sci. World J.* **2014**, *2014*, 10. [CrossRef]
25. Noh, Y.; Lee, U.; Wang, P.; Choi, B.S.C.; Gerla, M. VAPR: Void-aware pressure routing for underwater sensor networks. *IEEE Trans. Mob. Comput.* **2012**, *12*, 895–908 [CrossRef]
26. Ali, T.; Jung, L.T.; Faye, I. Delay efficient Layer by Layer Angle Based Flooding Protocol (L2-ABF) for Underwater Wireless Sensor Networks. Available online:https://pdfs.semanticscholar.org/64bb/2e8bdd2d526d141a13e4d2fdd46ff5e4a747.pdf(accessed on 18 June 2020)
27. Hafeez, T.; Javaid, N.; Hameed, A.R.; Sher, A.; Khan, Z.A.; Qasim, U. AVN-AHH-VBF: Avoiding void node with adaptive hop-by-hop vector based forwarding for underwater wireless sensor networks. In Proceedings of the 2016 10th International Conference on Innovative Mobile and Internet Services in Ubiquitous Computing (IMIS), Fukuoka, Japan, 6–8 July 2016; IEEE: Piscataway, NJ, USA, 2016; pp. 49–56.
28. Javaid, N. *NADEEM: Neighbor-Node Approaching Distinct Energy Efficient Mates for Reliable Dat a Delivery in IoT Enabled Underwater WSNs*; Transactions on Emerging Telecommunications Technologies (ETT): Beijing, China, 2019.
29. Farooq, W.; Ali, T.; Shaf, A.; UMAR, M.; Yasin, S. Atomic-shaped efficient delay and data gathering routing protocol for underwater wireless sensor networks. *Turk. J. Electr. Eng. Comput. Sci.* **2019**, *27*, 3454–3469. [CrossRef]
30. Yan, H.; Shi, Z.J.; Cui, J.H. DBR: Depth-based routing for underwater sensor networks. In *International Conference on Research in Networking*; Springer: Berlin/Heidelberg, Germany, 2008; pp. 72–86.
31. Wahid, A.; Lee, S.; Kim, D. A reliable and energy-efficient routing protocol for underwater wireless sensor networks. *Int. J. Commun. Syst.* **2014**, *27*, 2048–2062. [CrossRef]
32. Ali, T.; Jung, L.T.; Faye, I. Three hops reliability model for underwater wireless sensor network. In Proceedings of the 2014 International Conference on Computer and Information Sciences (ICCOINS), Kuala Lumpur, Malaysia, 3–5 June 2014; IEEE: Piscataway, NJ, USA, 2010; pp. 1–6.
33. Ayaz, M.; Abdullah, A.; Faye, I. Hop-by-hop reliable data deliveries for underwater wireless sensor networks. In Proceedings of the 2010 International Conference on Broadband, Wireless Computing, Communication and Applications, Fukuoka, Japan, 4–6 November 2010; IEEE: Piscataway, NJ, USA, 2010; pp. 363–368.
34. Domingo, M.C.; Prior, R. Energy analysis of routing protocols for underwater wireless sensor networks. *Comput. Commun.* **2008**, *31*, 1227–1238. [CrossRef]